Available online at www.sciencedirect.com

SCIENCE DIRECT®

Optics Communications 215 (2003) 101–111

OPTICS COMMUNICATIONS

www.elsevier.com/locate/optcom

Quantum analysis of the nondegenerate optical parametric amplifier with injected signal

M.K. Olsen [a,*], L.I. Plimak [b], A.Z. Khoury [a]

[a] *Instituto de Física da Universidade Federal Fluminense, Boa Viagem Cep.: 24210-340, Niterói, Rio de Janeiro, Brazil*

[b] *Fachbereich Physik, Universität Kaiserslautern, 67663 Kaiserslautern, Germany*

Received 16 October 2002; accepted 26 November 2002

Abstract

We perform a fully quantum analysis of the continuously pumped nondegenerate travelling wave optical parametric amplifier (NOPA), in both the spontaneous and stimulated regimes, using the positive-P representation. We find that an injected coherent signal at one of the lower frequencies can drastically increase the conversion efficiency, but at the expense of the quantum nature of the output fields. We show how the degree of violation of classical inequalities decreases as the injected signal is increased, and also as the propagation length increases. We also find that semiclassical solutions for the mean intensities become more accurate as the intensity of the injected signal increases.

PACS: 42.50.Ct; 42.65.Ky; 42.50.Dv; 42.50.Lc

Keywords: Quantum optics; Quantum correlations; Fully quantum analysis

1. Introduction

Among the simplest possible quantum optical systems which can exhibit nonclassical behaviour are travelling wave second harmonic generation and parametric downconversion. The process of travelling wave downconversion, achieved using an optical parametric amplifier, is of special interest because it allows for many experiments concerned with the fundamentals of quantum mechanics. Among these are violations of Bell's inequalities [1–3] and the closely related topic of preparation of Einstein–Podolsky–Rosen states [4,5]. The systems of degenerate and nondegenerate downconversion are often treated theoretically using the nondepleted pump approximation [4,6], which treats the input pump field as constant as it traverses the crystal. This approximation is even more of a simplification than the linearised analysis commonly used in travelling wave second harmonic generation (SHG), where the field amplitudes are treated as classical variables, and leads to solutions for the fields which clearly violate energy conservation [7,8]. The validity of this approach relies on the violation being negligible,

* Corresponding author. Tel.: +5521-2620-6735; fax: +5521-2620-3881.

E-mail address: mko@if.uff.br (M.K. Olsen).

0030-4018/02/$ - see front matter
PII: S0030-4018(02)02235-6

which restricts its usefulness to very small interaction lengths and efficiencies. As even linearisation has been shown to make misleading predictions for these parametric optical processes [9,10], we may suspect that the full quantum properties of the nondegenerate travelling wave optical parametric amplifier (NOPA) should be taken into account in a careful analysis. In a previous paper [11] we showed how the statistics of the input fields can effect both the intensities and the quantum statistics in travelling wave SHG and nondegenerate downconversion. In this work we investigate the effects of an auxiliary coherent signal field on the output fields of the NOPA, showing how conversion efficiency can be dramatically increased, but at the expense of the nonclassical properties of the fields. As an injected signal is commonly used in experiments to increase the conversion efficiency, it is of some interest to quantify these effects. We use a three-mode approach, which is justified by the fact that, with a macroscopic injected signal, stimulated downconversion dominates over spontaneous processes into other modes. Even though the latter are still present, they happen at a much lower rate, which will become even more insignificant as the signal intensity is increased. We give predictions without injected signal merely for the purposes of comparison, as our three-mode approximation is not expected to be valid in this regime.

We follow the approach of Huttner et al. [12], quantising the three interacting fields in terms of the photon fluxes rather than in terms of energy densities. This removes the problem of the requirement that each mode should be quantised in a different volume in a material whose refractive index is frequency dependent. Once we have found the appropriate momentum operator, we use the well-known mapping onto stochastic differential equations in the positive-P representation [13] to calculate the development of the fields as they traverse the medium. This gives access to any normally ordered operator moments without making any semiclassical approximations with respect to the three interacting electromagnetic fields. This approach has previously been used to calculate quantum properties of a similar system without an injected signal [14,15].

In the OPA, naive conversion of the operator equations of motion to c-number equations for the amplitudes predicts that, with vacuum inputs for the two lower frequency fields, no interaction can take place. We therefore also present an implicit solution for the intensities, which is reminiscent of earlier analyses in terms of Jacobi elliptic functions [6] for three-wave mixing processes with an injected signal, valid for a perfectly phase-matched system where we can ignore group velocity dispersion. This begins with the Heisenberg propagation equations of motion for the field intensities and goes one step past the usual linearised solutions in that it includes some of the quantum properties of the input states. We show how this "semiquantum" approach becomes more accurate as the amplitude of the injected signal is increased.

2. The system and equations of motion

The system of interest couples three electromagnetic fields via a nonlinear medium (normally a crystal), with a second-order susceptibility represented by $\chi^{(2)}$. The medium is pumped with a continuous wave laser at a frequency ω_c and has a much weaker coherent input signal, with frequency ω_b. Given the correct phase-matching conditions, this signal field stimulates the production of pairs of photons at the frequencies ω_b and ω_a, with $\omega_c = \omega_a + \omega_b$. Assuming that the stimulated rate is much higher than the spontaneous rate, which produces photon pairs at a range of different frequencies summing to ω_c, we will neglect the downconverted fields which are produced spontaneously. We can make an estimate of the validity of this approximation by considering that spontaneous downconversion is actually stimulated by the average energy of half a vacuum photon in each mode. Hence the rate with injected signal will be higher than this by a factor of $2n + 1$, with n being the average number in the signal. For the lowest intensity of injected signal that we consider here, this is a factor of 21. We consider here the case of one-dimensional propagation, which is valid for the case of colinear pumping. To avoid the problem of changes in quantisation volume when the refractive indices are frequency dependent, we follow the approach of Huttner et al. [12] and work in terms of fluxes. In this approach, the operator

$$\hat{N}(z_0, \omega_m) \equiv \hat{a}^\dagger(z_0, \omega_m)\hat{a}(z_0, \omega_m), \quad (1)$$

for example, is the number operator for photons at frequency ω_m which pass through a plane at $z = z_0$ during a time interval T, which remains undefined at this stage. Multiplying by the energy of the photons at each frequency and summing over the frequencies gives the total energy passing through the plane in this time T. The operators $\hat{a}^\dagger(z, \omega_m)$ and $\hat{a}(z, \omega_m)$ obey spatial commutation relations (see also Caves and Crouch [16])

$$[\hat{a}(z, \omega_i), \hat{a}^\dagger(z, \omega_j)] = \delta_{ij}. \quad (2)$$

This approach allows us to define the linear free-space momentum operator

$$\hat{G}_l(z) = \sum_m \hbar k_m \hat{a}^\dagger(z, \omega_m)\hat{a}(z, \omega_m), \quad (3)$$

where $k_m = \omega_m/c$ is the free-space wave vector. The above operator is actually the integral of a momentum flux operator over a period T, and can be seen to be the number of photons times their individual momentum, thus giving the total momentum of the field passing through the plane during the period of time considered.

Inside the nonlinear medium, and assuming phase-matching at the central frequencies of the three fields, i.e., $n(\omega_a) = n(\omega_b) = n(\omega_c)$, the nonlinear momentum operator is

$$\begin{aligned}\hat{G}_{nl}(z) = \sum_m \frac{\mathrm{i}\hbar\lambda(\epsilon_m)}{2} \Big[&\hat{a}(z, \omega_a + \epsilon_m) \\ &\times \hat{b}(z, \omega_b - \epsilon_m)\hat{c}^\dagger(z, \omega_c) \\ &- \hat{a}^\dagger(z, \omega_a + \epsilon_m)\hat{b}^\dagger(z, \omega_b - \epsilon_m)\hat{c}(z, \omega_c)\Big],\end{aligned} \quad (4)$$

where

$$\lambda(\epsilon_m) = \frac{\chi^{(2)}}{\epsilon_0 c}\left[\frac{(\omega_a + \epsilon_m)(\omega_b - \epsilon_m)}{n(\omega_a + \epsilon_m)n(\omega_b - \epsilon_m)}\right]^{1/2}. \quad (5)$$

Note that the frequency of the pump field, represented by the operator $\hat{c}(z, \omega_c)$, is fixed. We consider that this is a justifiable approximation, at least until the point where there is significant recombination of the two lower frequency fields.

As shown by Shen [17], we can now write an equation of motion for the density matrix of the system

$$\mathrm{i}\hbar\frac{\partial\rho(z)}{\partial z} = \left[\rho(z), \hat{G}_{nl}(z)\right]. \quad (6)$$

This equation allows for the calculation of steady-state propagation in the medium, which is exactly what we require for continuous pumping. Physically, the density matrix, $\rho(z)$, describes an ensemble of steady-state systems which has all the statistical properties of the fields at point z. Hence Eq. (6) provides a full description of the interacting fields. Unfortunately, as it is a nonlinear operator equation, it is, at the very least, extremely difficult to solve. A commonly used method is to linearise the equations around the semiclassical mean values of the operators, and solve the resulting c-number equations. This is not applicable in this situation as it predicts that, beginning with only the pump mode occupied, no interaction can take place. In some cases the master equation can be solved numerically using a truncated number state basis, but this necessarily restricts the number of interacting quanta that can be dealt with and would be impractical for the present case.

Hence we proceed by mapping the master equation onto the Fokker–Planck equation for the positive-P pseudoprobability distribution of the system. Following the usual methods [18], and setting $\kappa = \lambda(\epsilon_m)/2$, we find

$$\begin{aligned}\frac{\partial P}{\partial z} = \Bigg\{ &-\kappa\left[\frac{\partial}{\partial\alpha}\beta^+\gamma + \frac{\partial}{\partial\alpha^+}\beta\gamma^+ + \frac{\partial}{\partial\beta}\alpha^+\gamma + \frac{\partial}{\partial\beta^+}\alpha\gamma^+ \right.\\ &\left.+ \frac{\partial}{\partial\gamma}(-\alpha\beta) + \frac{\partial}{\partial\gamma^+}(-\alpha^+\beta^+)\right] \\ &+ \frac{2\kappa}{2}\left[\frac{\partial^2}{\partial\alpha\partial\beta}\gamma + \frac{\partial^2}{\partial\alpha^+\partial\beta^+}\gamma^+\right]\Bigg\} \\ &\times P(\alpha, \alpha^+, \beta, \beta^+, \gamma, \gamma^+, z).\end{aligned} \quad (7)$$

In the above equation, there is a correspondence between the c-number variables (α, β, γ) and the operators $(\hat{a}, \hat{b}, \hat{c})$. Note that we are no longer summing over the ϵ_m, but are now considering that we are dealing with modes whose bandwidths will be set by the two input lasers. We are assuming that these bandwidths are narrow enough that they can be regarded as monochromatic and hence each can be described as a single propagating field. One possible factorisation of the diffusion matrix of Eq. (7) leads to the following set of coupled stochastic differential equations in Itô calculus [18]

$$
\begin{aligned}
\frac{d\alpha}{dz} &= \kappa\beta^{+}\gamma + \sqrt{\frac{\kappa}{2}}\gamma(\eta_1(z) + i\eta_2(z)),\\
\frac{d\alpha^{+}}{dz} &= \kappa\beta\gamma^{+} + \sqrt{\frac{\kappa}{2}}\gamma^{+}(\eta_3(z) + i\eta_4(z)),\\
\frac{d\beta}{dz} &= \kappa\alpha^{+}\gamma + \sqrt{\frac{\kappa}{2}}\gamma(\eta_1(z) - i\eta_2(z)),\\
\frac{d\beta^{+}}{dz} &= \kappa\alpha\gamma^{+} + \sqrt{\frac{\kappa}{2}}\gamma^{+}(\eta_3(z) - i\eta_4(z)),\\
\frac{d\gamma}{dz} &= -\kappa\alpha\beta,\\
\frac{d\gamma^{+}}{dz} &= -\kappa\alpha^{+}\beta^{+},
\end{aligned} \tag{8}
$$

where the η_i are real noise terms with the correlations $\overline{\eta_i(z)\eta_j(z')} = \delta_{ij}\delta(z - z')$. As always with the positive-P, the pairs of field variables (α and α^{+} for example) are not complex-conjugate except in the mean of a large number of integrated trajectories. It is of interest here that image transfer experiments with this system demonstrate that an image transferred by the input of field β, for example, is perceived as the complex-conjugate in output field α [19]. Examining the noise terms in Eq. (8), we see that there is a partial complex conjugation between the fields α and β. We also note here that the above equations, while written in a slightly different form, are completely equivalent to those of [14].

We are particularly interested here in a system where $\gamma(0) \neq 0$ and $\beta(0) \neq 0$, but $\alpha(0) = 0$. The field represented by $\beta(0)$ is the injected signal, which is commonly used to increase the conversion efficiency. We will examine below the extent to which quantum correlations between the two output fields are preserved as the injected signal becomes more intense and how violations of classical inequalities are affected. However, we will first examine the solutions for the mean-fields of the output intensities.

3. Semiquantum analytical solutions for the intensities

What we may call the semiclassical solutions for the system of spontaneous nondegenerate down-conversion follow from setting the noise terms in Eq. (8) to zero. This leaves us with three coupled equations for the complex field amplitudes α, β and γ. It is obvious by inspection that, for initial conditions $\alpha(0) = \beta(0) = 0$ and $\gamma(0) \neq 0$, the solutions for all z remain identical to the initial conditions. This is because the process of spontaneous down-conversion is noise-driven and cannot begin with the two lower frequency modes being considered as being in classical vacuum states. Indeed we may think of it as a process which is stimulated by vacuum fluctuations, which is readily seen if the equations of motion are written in the Wigner representation [20], where the initial conditions for the modes include the vacuum fluctuations. Considering the semiclassical equations of motion with $\beta(0) \neq 0$, that is, with an injected signal, we see that

$$
\left.\frac{d\alpha}{dz}\right|_{z=0} = \kappa\beta^{*}(0)\gamma(0) \neq 0, \tag{9}
$$

so that, with injected signal, the process no longer relies on fluctuations to proceed.

However, by going one step further, as done previously for travelling wave SHG [9,21] and third harmonic generation [22], and deriving equations of motion for the mean values of the field *intensity* operators, we find nontrivial solutions even without an injected signal. As with SHG, we find that these solutions, while an improvement over the semiclassical solutions for the amplitudes, are at best only partially accurate for small injected signals. Physically, as the injected signal strength decreases, we enter the region where we would not expect our three-mode model to be accurate, as spontaneous pair production can occupy other modes in a way that is not included in our equations. We will therefore develop the equations including the effects of the signal injection, with the caveat that the solutions have no physically meaningful limit as this goes to zero.

Writing the field intensity operators as $\hat{N}_j$ (where $j = a, b, c$), we find the equation of motion for the operator $\hat{N}_c$ as

$$i\hbar\frac{d\hat{N}_c}{dz} = \left[\hat{G}_{nl}(z), \hat{N}_c\right], \tag{10}$$

which gives

$$\frac{d\hat{N}_c}{dz} = -\kappa\left(\hat{a}^\dagger\hat{b}^\dagger\hat{c} + \hat{a}\hat{b}\hat{c}^\dagger\right), \tag{11}$$

which still has no obvious solution. In fact, the semiclassical solution of this equation still says that the process cannot proceed, even with injected signal, as $\langle\hat{a}(0)\rangle = \langle\hat{a}^\dagger(0)\rangle = 0$. However, proceeding further and taking the second derivative, we find

$$\frac{d^2\hat{N}_c}{dz^2} = 2\kappa^2\left[\hat{N}_a\hat{N}_b - \hat{N}_c\left(\hat{N}_a + \hat{N}_b + 1\right)\right]. \tag{12}$$

As a nonlinear operator equation, this equation is, at the very least, extremely difficult to solve analytically.

What we do see is that if we assume all operator products factorise and take the semiclassical solutions for the expectation values at $z = 0$ without injected signal, we find that

$$\left.\frac{d^2N_c}{dz^2}\right|_{z=0} = -2\kappa^2 N_c(0), \tag{13}$$

where $N_c = \langle\hat{N}_c\rangle$. As this is negative, we see that N_c will decrease, so that the process may now proceed and we can find an implicit analytical solution which we shall call semiquantum, in view of the fact that we have now included some quantum effects, at least in the initial conditions.

For the fully spontaneous process, only $N_c(0)$ is nonzero and for every photon created in mode a, a photon is created in mode b, due to the annihilation of a photon in mode c. This allows us to write the following relation:

$$N_a(z) = N_b(z) = N_c(0) - N_c(z), \tag{14}$$

so that, letting $N_c(0) = N_0$ and $N_c(z) = N_c$, we would be able to write a second-order differential equation for $N_c(z)$. We are, however, more interested in the general case where $N_b(0) \neq 0$, which exhibits different conservation relations

$$N_a(z) = N_b(z) - N_b(0) = N_c(0) - N_c(z), \tag{15}$$

so that we may make the substitutions

$$\begin{aligned} N_a(z) &\to N_c(0) - N_c(z), \\ N_b(z) &\to N_b(0) + N_c(0) - N_c(z). \end{aligned} \tag{16}$$

We see from these relations that, semiclassically, the number difference $N_b - N_a$ would exhibit perfect squeezing, remaining constant throughout the propagation. We will check the accuracy of this prediction below, using a fully quantum analysis.

Writing $C = N_c(0)$ and $B = N_b(0)$, we find the following second-order differential equation for $N_c(z)$:

$$\frac{d^2N_c}{dz^2} = 2\kappa^2\left[3N_c^2 - (2B + 4C + 1)N_c + C(B + 1)\right]. \tag{17}$$

As done previously in [9,21,22], we may regard this equation as equivalent to Newton's second law for one-dimensional motion in a pseudopotential, with N_c being the coordinate. We therefore write

$$\frac{d^2N_c}{dz^2} = -\frac{\partial U(N_c)}{\partial N_c}. \tag{18}$$

The pseudopotential $U(N_c)$ is found by straightforward integration

$$\begin{aligned} U(N_c) = -2\kappa^2\Bigg[N_c^3 - \left(B + 2C + \frac{1}{2}\right)N_c^2 \\ + (BC + C^2)N_c + D\Bigg], \end{aligned} \tag{19}$$

where D is an arbitrary constant which we may set equal to zero. This leads immediately to

$$\frac{d}{dz}\left[\frac{1}{2}\left(\frac{dN_c}{dz}\right)^2\right] = -\frac{dU}{dz}, \tag{20}$$

so that

$$\frac{1}{2}\left(\frac{dN_c}{dz}\right)^2 + U(N_c) = E \tag{21}$$

is a constant of the motion which we may consider as a sum of kinetic and potential pseudoenergies. It is easily seen that $E = U(C)$ without injected signal.

The shape of this pseudopotential, shown in Fig. 1 for different values of injected signal, will obviously lead to a periodic behaviour of the photon number. What we see is that the injected signal does not drastically change the form of the pseudopotential until its value becomes reasonably large (≈10%) of the pumping at the high frequency mode. Noting that the motion of N_c begins on the

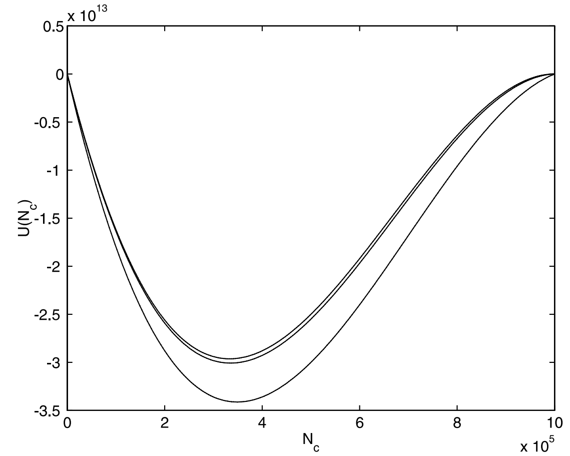

Fig. 1. Pseudopotentials in which N_c undergoes periodic motion in the "semiquantum" analysis, for parameters $N_c(0) = 10^6$, $N_a(0) = 0$ and $\kappa = 10^{-2}$, the same as used in subsequent figures. The curves are for $N_b(0) = 0$, $0.01 \times N_c(0)$ and $0.1 \times N_c(0)$, in descending order. Note that the motion begins on the right-hand side of the potential.

right-hand side of the graph, what we do see with an injected signal is that the derivative of the potential at this point increases in magnitude as the signal increases, meaning that the injected signal has the effect of adding kinetic pseudoenergy at the beginning of the process. We would thus expect to see significant conversion for shorter interaction lengths as the signal was increased.

Using Eqs. (21) and (19) leads immediately to an equation for the first derivative

$$\frac{dN_c}{dz} = \pm 2\kappa \left\{ \frac{E}{\kappa^2} + N_c^3 - (B + 2C + 1/2)N_c^2 + (BC + C^2)N_c \right\}^{1/2}, \quad (22)$$

which has the implicit solution

$$z = \pm \frac{1}{2\kappa} \int_{N_c(0)}^{N_c(z)} dN_c \Big/ \left(N_c^3 - (B + 2C + 1/2)N_c^2 + (BC + C^2)N_c + E/\kappa^2 \right)^{1/2}, \quad (23)$$

which can alternatively be written as

$$z = \pm \frac{1}{\kappa} \int_{N_0}^{N_c} dN_c \Big/ \left(\sqrt{(N_c - N_1)(N_c - N_2)(N_c - N_3)} \right), \quad (24)$$

where the N_j are the roots of the polynomial expression in Eq. (23). Although explicit solutions for the intensities can be developed in terms of Jacobi elliptic functions, they are not very informative. Therefore we shall content ourselves with having shown that an analytical periodic solution exists and will proceed to compare numerical solutions of the equations of motion with solutions obtained quantum mechanically, via stochastic integration.

4. The mean fields

The solution of the previous section, even though it used at least some of the quantum properties of the input fields, does not allow us to calculate anything about the quantum statistics of the output fields. Therefore we resort to numerical stochastic integration of Eq. (8), which, as long as the integration converges, gives access to any desired operator moments. Firstly, in this section, we will investigate the effect of the auxiliary injected signal on the output fields and show how, as the signal is augmented, the quantum solutions approach those obtained semiclassically. As stated above, the quantum solutions without injected signal are shown only for purposes of comparison. They are not expected to be accurate physically, as many modes which are not present in our equations would be involved. Even though this is, strictly speaking, still the case with an injected signal, the stimulated process is so much stronger than the spontaneous process that we expect the approximation of only three interacting modes to be valid, at least up to the point where the downconverted fields begin to recombine and the upconversion process begins to dominate.

In Fig. 2 we show the positive-P solutions for the fully spontaneous process, calculated using 2.3×10^5 stochastic trajectories, as compared to the semiquantum solutions. In all results given in this paper we have used initial conditions of $\kappa = 0.01$, $|\gamma(0)|^2 = 10^6$ and $|\alpha(0)|^2 = 0$. For the spontaneous process, $|\beta(0)|^2$ is also zero. The results are given as functions of a scaled interaction length, $\xi = \kappa|\gamma(0)|z$. Note that the semiquantum solutions closely follow the quantum solutions at

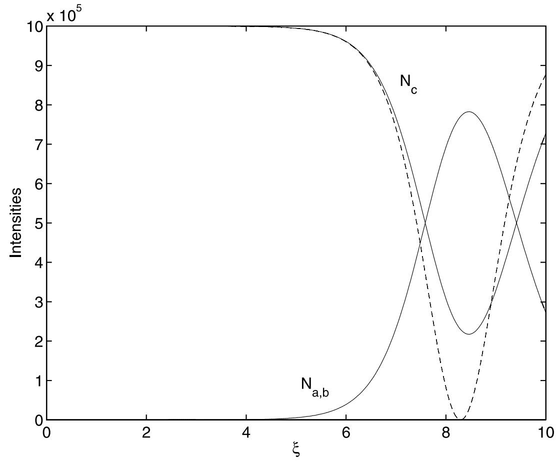

Fig. 2. The "semiquantum" and quantum solutions for field intensities in the fully spontaneous process. The "semiquantum" solution for N_c is given by the dash-dotted line. The x-axis is a scaled dimensionless interaction strength, $\xi = \kappa|\gamma(0)|z$. The values of κ, $N_c(0)$ and $N_a(0)$ are as in Fig. 1. In all graphs, signal intensities should be considered in relation to $N_c(0)$.

the beginning of the interaction, but exhibit a much more complete conversion to the low frequency modes. The quantum prediction in this case is for ≈80% conversion of the pump field. This is reminiscent of the case of travelling wave SHG [9], where similar semiquantum solutions showed a clear periodicity, whereas the quantum solutions did not. A similar difference between quantum and semiquantum/semiclassical predictions has been seen in the case of photoassociation of Bose–Einstein condensates [23], where the predictions of the Gross–Pitaevski equation are accurate only for a short time. It is interesting to note that the addition of a $\chi^{(3)}$ component to the travelling wave SHG interaction brings the quantum and semiclassical solutions into a much better agreement [21,24]. Whether this is also the case here is subject to further investigation. The difference between the solutions for these parameters can be explained by the lack of phase coherence in the quantum field amplitudes. In other words, as the downconversion process is spontaneous there is no phase reference. When the amplitudes of all three fields are positive, the two low frequency fields increase while the pump field decreases, as can be seen by inspection of the equations of motion. As soon as the product $\alpha\beta$ attains a negative value, the pump field will start to rise again and the lower frequency fields will decrease. This is the same reason why, in travelling wave SHG, a full conversion to the harmonic is not found after the first minimum.

Once a coherent signal is injected, i.e., $|\beta(0)|^2 > 0$, we may directly solve the semiclassical equations of motion for the field amplitudes and find conversion. Interestingly enough, any nonzero value of the signal results in total conversion in the semiclassical predictions. For the positive-P representation simulations, we averaged over 3.7×10^5 trajectories ($N_b(0) = 10^{-5}N_c(0)$ and $10^{-3}N_c(0)$) and 2.2×10^5 trajectories ($N_b(0) = 10^{-1}N_c(0)$). For a signal to pump intensity ratio of 10^{-6} (averaged over 2.8×10^5 trajectories), the quantum prediction is for a conversion efficiency not very different to that of the spontaneous process. The mean field equations, integrated numerically, show complete conversion with the first minimum in $|\gamma(0)|^2$ a little after the quantum prediction. As can be seen in Fig. 3, with an input signal intensity of 10^{-5} times the pump intensity, the predictions of the quantum mechanical and semiclassical approaches have become closer, with a more

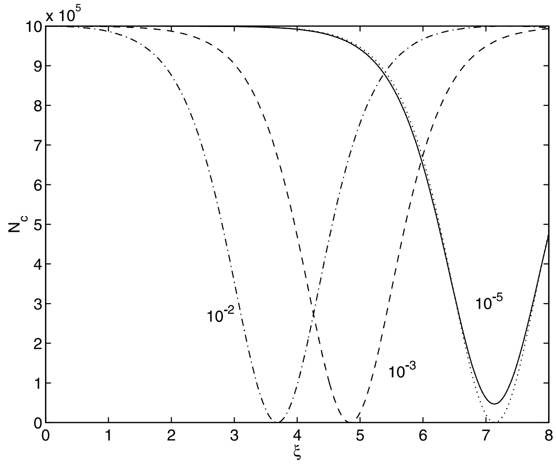

Fig. 3. Solutions for the N_c with different injected signal intensities. For a signal strength $N_b(0) = 10^{-5} \times N_c(0)$, we show the quantum solution (full-line) and the "semiquantum" solution (dotted line). For the higher signal strengths, the solutions are indistinguishable. The values of κ, $N_c(0)$ and $N_a(0)$ are as in Fig. 1.

complete conversion from the high frequency field. The fact that we do not see full conversion in the quantum mechanical result indicates that there is still a significant spontaneous component to the process for this signal strength. Also, as the input signal increases, the interaction length required to see the first minimum decreases. As the signal intensity is increased further, the two predictions become indistinguishable and the period decreases, as can readily be seen in the figure. This is an indication that the whole process is in some respect becoming more classical as the stimulated process begins to dominate. In the next section we investigate what effect the strength of the signal may have on various quantum correlations and quantify how the output fields become less quantum as the signal increases.

5. Quantum correlations

Semiclassical, linearised analyses predict that the system of nondegenerate downconversion will exhibit increasingly quantum features, such as entanglement, violation of Bell's inequalities and perfect difference quadrature squeezing, as the conversion efficiency is increased. These predictions are generally made using the undepleted pump approximation and can therefore be expected to have only limited validity. A previous fully quantum analysis [14,15] has shown that the positive-P predictions, particularly for phase quadrature squeezing, differ from those of various other methods once a certain interaction efficiency is reached. This is also predicted to be the case in travelling wave SHG, where the undepleted pump approximation is not generally used [9]. In this paper, we will not compare the quantum predictions with those obtained by other approaches, but will focus on the effects of an injected coherent signal on various correlations.

We first investigate the variance in the difference between the two low frequency amplitude quadratures, $V(X_a - X_b)$, defined as

$$V(X_a - X_b) = \frac{1}{2}\left(\langle : (X_a - X_b)^2 : \rangle - \langle X_a - X_b \rangle^2\right), \tag{25}$$

so as to exhibit a value of unity for two uncorrelated coherent states. Note here that we use the definition $X = \hat{a} + \hat{a}^\dagger$. Any value of less than one means that these two quadratures have become more correlated during the propagation than they were at the start of the interaction. Using the undepleted pump approximation, this variance is calculated to go to zero in the spontaneous process. The positive-P predictions in this case show that a value very close to zero (<0.01) is attained over a certain range, but the variance begins to increase as the conversion from the high frequency field becomes noticeable. As stated previously, all results for the spontaneous process are merely for purposes of comparison. In Fig. 4 we show the predictions for three different values of injected signal. As this is increased, the minimum value of the variance increases, although only slightly until we are injecting a signal with approximately one-tenth the intensity of the coherent pump. This is because the injected field adds a coherent part to the propagating field, $\beta(z)$, so that it is no longer composed only of photons which are formed jointly with those in the other low frequency field. What we also see is that this variance reaches a minimum and begins to increase as the process of recombination to form higher frequency photons

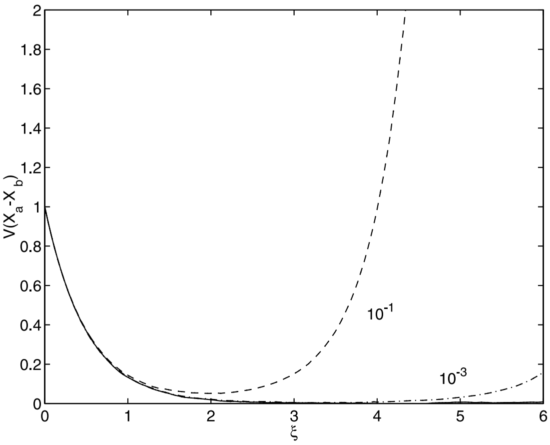

Fig. 4. The behaviour of $V(X_a - X_b)$ as the signal strength is increased. The numbers on the graph refer to the ratio of the injected signal intensity to the pump. The lower line, which stays very near the ξ-axis, represents a signal of 10^{-5} times the pump intensity. The values of κ, $N_c(0)$ and $N_a(0)$ are as in Fig. 1.

becomes predominant. This is reminiscent of a similar effect predicted for travelling wave SHG [25] and can be explained by the fact that photons with different phases are combining at this stage of propagation, meaning that the fields are losing their phase reference. The complementary quadrature, $Y_a - Y_b$, always exhibits a large degree of antisqueezing.

Another quantum correlation which the undepleted pump approximation predicts to be perfect in the spontaneous process is what we may call the Fano factor of the number difference between the two low frequency modes, defined as $F(N_a - N_b) = V(N_a - N_b)/(N_a + N_b)$, which again has a value of one for two coherent states. As stated in Section 3, this perfect correlation, or the fact that $N_b - N_a$ is a constant in the semiclassical approach, was used to develop the semiquantum analytical solutions for N_c. In Fig. 5 we see that this correlation exhibits a similar behaviour to $V(X_a - X_b)$ as a function of the injected signal, showing a large degree of compression over some range of propagation length. Here the fact that the Fano factor increases with the signal intensity can be explained by the number uncertainty of the injected coherent state, which exhibits Poissonian number statistics. As the signal increases, this uncertainty becomes more

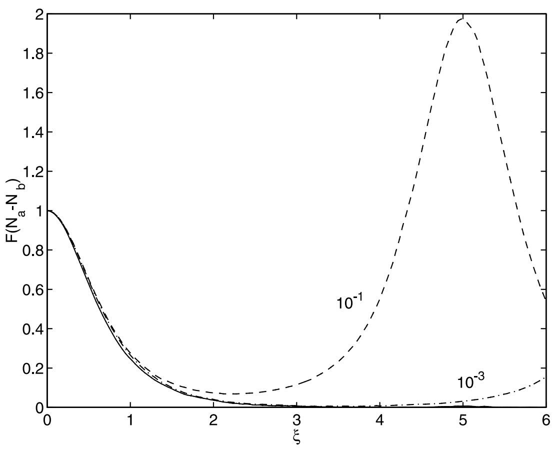

Fig. 5. The behaviour of $F(N_a - N_b)$ as the signal is increased, with the numbers representing the ratio of signal intensity to pump intensity. The result for a signal of 10^{-5} times the pump intensity stays very near the ξ-axis. The values of κ, $N_c(0)$ and $N_a(0)$ are as in Fig. 1.

important than the number uncertainty in the downconverted modes. We again see an increase in this variance as the two low frequency modes begin to recombine.

We may also write a Cauchy–Schwarz inequality for the two low frequency fields

$$\langle \hat{a}^{\dagger 2}\hat{a}^2\rangle\langle \hat{b}^{\dagger 2}\hat{b}^2\rangle \geqslant \langle \hat{a}^\dagger\hat{a}\hat{b}^\dagger\hat{b}\rangle^2, \tag{26}$$

which may not be violated by fields with a positive Glauber P-function. Hence any violation means that the two fields are more quantum than the coherent states, which are sometimes thought of as defining the boundary between classical and quantum behaviour. In the present situation though, it is worth noting that the use of the truncated Wigner representation for this system gives predictions equivalent to those of the positive-P for the correlations we have calculated. This indicates that violation of classical inequalities is possible for systems with a positive Wigner function (whereas the boundary between positive and negative Wigner functions is sometimes used for the definition of the division between classical and nonclassical behaviour, especially using the theory of stochastic electrodynamics [26]). Rewriting the above inequality as a correlation function, we have

$$\frac{\langle \hat{a}^{\dagger 2}\hat{a}^2\rangle\langle \hat{b}^{\dagger 2}\hat{b}^2\rangle}{\langle \hat{a}^\dagger\hat{a}\hat{b}^\dagger\hat{b}\rangle^2} \geqslant 1, \tag{27}$$

so that any value of less than one indicates nonclassical behaviour. In Fig. 6 we show that this correlation between the two fields also becomes more classical as the intensity of the injected coherent signal increases. Interestingly, even with no injected signal, the maximum violation is seen for shorter interaction lengths, which is consistent with published results which reported that violations of local realism were more pronounced for smaller values of r, where r is the amplification parameter of the idler field [3]. The value of this correlation at the input is one, which is not well shown on the graph. What can be seen is that the value for the spontaneous process reports the maximum violation of the inequality as soon as conversion begins. This is due to the fact that twin photons are produced immediately, albeit with a low efficiency, representing a type of phase transition between two uncorrelated vacuums and two

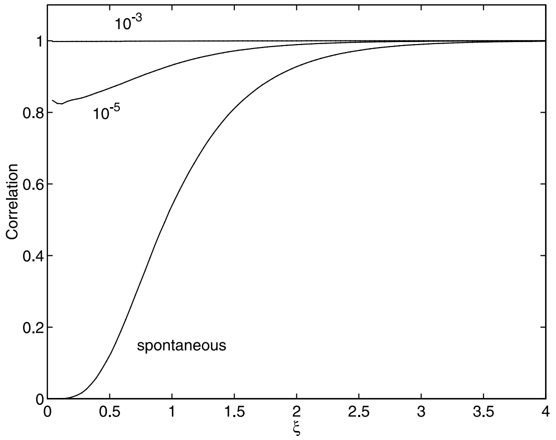

Fig. 6. Violation of the Cauchy–Schwarz inequality with injected signal. The numbers on the graph refer to the ratio of the signal to the pump intensity. Any value of less than one for the correlation is impossible for fields which have a representation in terms of a positive Glauber P-function. The values of κ, $N_c(0)$ and $N_a(0)$ are as in Fig. 1.

fully correlated photons. When we inject a signal, we are essentially adding a coherent state component to one of the fields. Even though this coherent state itself interacts with the crystal, it has a representation as a positive P-function (in fact a Dirac delta) and cannot violate the inequality. We therefore see less violation of this inequality, and may consider that the signal field now has two components; one of which may violate the inequality and one of which may not. What is seen is that the degree of violation of this inequality is much more sensitive to the intensity of the injected signal than are the quadrature and number difference variances considered above. With an injected signal of only 0.1% of the pump intensity, there is negligible violation.

6. Conclusion

Using fully quantum propagation equations, we have shown that an injected coherent signal in the process of nondegenerate travelling wave parametric downconversion can dramatically increase the conversion efficiency. We have also quantified the effect of the injected signal on the quantum statistics of the interacting fields, showing how there is a loss in some of the more quantum features of the system. We have also shown that semiclassical and semiquantum mean field solutions to the equations of motion are not accurate for arbitrary interaction lengths with small values of the injected signal. As the signal increases, the agreement between the quantum and semiclassical mean field solutions improves, due to the fact that stimulated processes due to the injected coherent signal begin to dominate over spontaneous processes. As in travelling wave SHG, we show that predictions that quantum properties will improve with propagation length are not accurate, which is in agreement with experimental findings. Our analysis in terms of colinear propagation of the three fields should retain validity for interaction lengths less than the Rayleigh lengths of the interacting fields, so that diffraction processes within the crystal do not play a significant role. The analysis in terms of three interacting modes is expected to be valid until upconversion begins to play a significant role in the process.

Acknowledgements

This research was supported by the New Zealand Foundation for Research, Science and Technology (UFRJ0001), the Brazilian agency CNPq (Conselho Nacional de Desenvolvimento Científico e Tecnológico) and the Deutsche Forschungsgemeinschaft under contract FL210/11.

References

[1] Z.Y. Ou, L. Mandel, Phys. Rev. Lett. 61 (1988) 50.
[2] P. Grangier, M.J. Potasek, B. Yurke, Phys. Rev. A 38 (1988) 3132.
[3] A. Kuzmich, I.A. Walmsley, L. Mandel, Phys. Rev. Lett. 85 (2000) 1349.
[4] M.D. Reid, Phys. Rev. A 40 (1989) 913.
[5] Z.Y. Ou, S.F. Pereira, H.J. Kimble, K.C. Peng, Phys. Rev. Lett. 68 (1992) 3663.
[6] J.R. Armstrong, N. Bloembergen, J. Ducuing, P.S. Pershan, Phys. Rev. 127 (1962) 1918.
[7] B.R. Mollow, R.J. Glauber, Phys. Rev. 160 (1967) 1076.
[8] B.R. Mollow, R.J. Glauber, Phys. Rev. 160 (1967) 1097.
[9] M.K. Olsen, R.J. Horowicz, L.I. Plimak, N. Treps, C. Fabre, Phys. Rev. A 61 (2000) 021803.

[10] M.K. Olsen, L.I. Plimak, M.J. Collett, D.F. Walls, Phys. Rev. A 62 (2000) 023802.
[11] M.K. Olsen, L.I. Plimak, A.Z. Khoury, Opt. Commun. 201 (2002) 373.
[12] B. Huttner, S. Serulnik, Y. Ben-Aryeh, Phys. Rev. A 42 (1990) 5594.
[13] P.D. Drummond, C.W. Gardiner, J. Phys. A 13 (1980) 2353.
[14] P. Kinsler, M. Fernée, P.D. Drummond, Phys. Rev. A 48 (1993) 3310.
[15] M. Fernée, P. Kinsler, P.D. Drummond, Phys. Rev. A 51 (1995) 864.
[16] C.M. Caves, D.D. Crouch, J. Opt. Soc. Am. B 4 (1987) 1535.
[17] Y.R. Shen, Phys. Rev. 155 (1967) 921.
[18] C.W. Gardiner, Quantum Noise, Springer, Berlin, 1991.
[19] P.H. Souto Ribeiro, D.P. Caetano, M.P. Almeida, J.A. Huguenin, B. Coutinho dos Santos, A.Z. Khoury, Phys. Rev. Lett. 87 (2001) 133602.
[20] M.K. Olsen, K. Dechoum, L.I. Plimak, Opt. Commun. 190 (2001) 261.
[21] V.I. Kruglov, M.K. Olsen, Phys. Rev. A 64 (2001) 053802.
[22] M.K. Olsen, L.I. Plimak, M. Fleischhauer, Phys. Rev. A 65 (2002) 053806.
[23] J.J. Hope, M.K. Olsen, Phys. Rev. Lett. 86 (2001) 3220.
[24] M.K. Olsen, V.I. Kruglov, M.J. Collett, Phys. Rev. A 63 (2001) 033801.
[25] M.K. Olsen, R.J. Horowicz, Opt. Commun. 168 (1999) 135.
[26] T.W. Marshall, Proc. R. Soc. London Ser. A 276 (1963) 475.